The Dynamics, Structure & History of Galaxies
ASP Conference Series, Vol. nnn, 2002
G. S. Da Costa & E. M. Sadler, eds

Star Formation in the Local Universe

Daniela Calzetti

Space Telescope Science Institute, 3700 San Martin Drive, Baltimore, MD 21218, U.S.A., calzetti@stsci.edu

Jason Harris

Space Telescope Science Institute, jharris@stsci.edu

Abstract. We present preliminary results of a long-term study aimed at answering a number of open questions on the evolution of starbursts in local galaxies. The project employes mainly HST data from the ultraviolet to the red of the stellar continuum and of the nebular emission from the galaxies. Here we concentrate on NGC5253 and NGC5236 (M83), that form a dwarf–massive galaxy pair at about 4 Mpc distance. The recent star formation history of the centers of the two galaxies is investigated in order to identify similarities and differences in the evolution of their central starbursts.

1. Introduction

Star formation is a driving force behind galaxy evolution; it largely determines the stellar, energy (radiant and mechanical), metal, and dust content of a galaxy. Throughout much of the history of the Universe, a significant fraction of the galaxy population is represented by galaxies undergoing intense star formation activity; at redshift z$\simeq$1 the star formation rate per unit comoving volume was roughly an order of magnitude higher than at present times (Lilly et al. 1996; Madau et al. 1996; Cowie, Songaila & Barger 1999). Yet, a number of questions related to the evolution of intense star formation episodes remain unresolved. Among them: (1) the duration, duty cycle, and star formation history of starbursts; (2) the importance of self-triggering and propagation for the evolution of the starburst (e.g., Walborn et al. 1999); (3) the impact of starbursts on the host galaxy's ISM and the feedback onto the evolution of the starburst itself; and (4) the possibility of distinct cluster and diffuse field star formation modes (Meurer et al. 1995).

In order to begin addressing these issues, we are undertaking a comprehensive study of $\sim$20 nearby (<20 Mpc) starburst galaxies covering a representative range of characteristics: morphological types ranging from dwarf irregulars (He 2-10) to grand-design spirals (M83); starburst star formation rates (SFR) from 0.1 $M_\odot$ yr^{-1} to 5 $M_\odot$ yr^{-1}; metallicities from 1/13 $Z_\odot$ to 2 $Z_\odot$; and dust attenuations in the range $0 \lesssim A_V \lesssim 3$. The data that are being collected for this study include HST ultraviolet and optical imaging in broad– and narrow–band filters of the stellar continuum and selected nebular emission lines (typi-

cally Hβ and Hα for dust reddening corrections and for tracing the ionized gas, [OIII](5007 Å) and [SII](6731 Å) for mapping of photo– and shock–ionized gas), ground–based optical imaging, and HST UV spectroscopy. In this contribution, we concentrate on the galaxy pair NGC5253–NGC5236, for which almost all needed data are available and the analysis is almost completed.

The two galaxies form an interesting, complementary pair in the Centaurus Group: NGC5253 is a dwarf galaxy that is about 10 times more metal poor ($\sim$1/5 $Z_\odot$) and about 100 times less massive ($\approx 10^9$ $M_\odot$) than its grand-design spiral companion NGC5236 (M83). The projected distance between the two galaxies is $\sim$130 kpc, and a close encounter between the two about 1–2 Gyr ago has been suggested as the initial trigger of the star formation in NGC5253 (Rogstad, Lockhart & Wright 1974; van den Bergh 1980; Caldwell & Phillips 1989). Despite the dissimilarities of the host galaxies, the central starbursts share some common properties: both have a SFR$\sim$0.2 $M_\odot$ yr^{-1} over an area of $\sim$400 pc in size; and both are characterized by patchy dust obscuration, with relatively transparent regions counterbalanced by highly opaque areas and dust lanes. However, while in NGC5253 star formation is diffused throughout the central region (Calzetti et al. 1997, and references therein), in NGC5236 star formation is concentrated in a semi–annulus centered on the optical nucleus, and has possibly been triggered by the galaxy's bar (Thatte et al. 2000; Harris et al. 2001).

Located at a distance of about 4 Mpc (Sandage et al. 1994), the two galaxies were imaged with the HST WFPC2 from the UV to the I-band (Calzetti et al. 1997, Harris et al. 2001), yielding a resolution of $\sim$1–2 pc per pixel, which is comparable to the typical half-light radius of stellar clusters. The UV–V–I colors of the central galaxies' regions, combined with the Hα emission map, were used to constrain the ages of the stellar populations, while Hα/Hβ ratio maps were used to remove the effects of dust reddening from the colors and luminosities. HST STIS long-slit UV spectra of the central region of NGC5253 were used to analyze in detail the characteristics of the hot star populations in this galaxy (Tremonti et al. 2001). Below is a summary of our current understanding of the star formation history in the centers of the two galaxies.

2. The Dwarf Galaxy NGC5253

The central region of active star formation in this galaxy is very blue at UV–optical wavelengths, except for a prominent dust lane with $A_V \gtrsim 2.2$ mag that bisects the starburst nearly perpendicularly to the galaxy's major axis (Calzetti et al. 1997; and Figure 1). The region contains about a dozen UV-bright stellar clusters, as well as diffusely distributed blue stars (Meurer et al. 1995). Radio observations, however, indicate that the bulk of the most recent star formation is hidden by dust (Turner, Ho & Beck 1998; Turner, Beck & Ho 2000). The distribution of the UV emission is slightly elongated along the major axis, and is markedly different from the morphology of the ionized gas emission (Hα); the latter is circularly symmetric about a bright stellar cluster close to the geometric center of the galaxy (NGC5253–5 of Calzetti et al. 1997, see Figure 1), and is about a factor of 2 more extended than the UV stellar continuum (Calzetti et al. 1999).

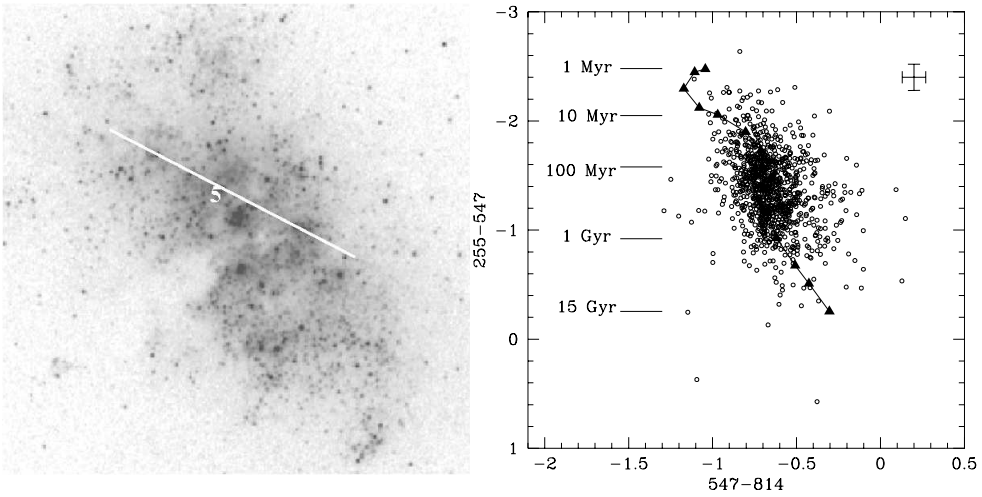

Figure 1: (left) The UV (2600 Å) WFPC2 image of the central starburst in NGC5253, showing the presence of a number of bright stellar clusters and of diffuse emission. The image has size 38″, which correspond to a physical size of ∼700 pc. The position of the STIS slit is shown as a thick line (Tremonti et al. 2001). The number '5' shows the position of the super-star-cluster candidate NGC5253-5, which has age $\lesssim$2 Myr and is at the center of the peak-activity region (Calzetti et al. 1997). North is up, East is left.

Figure 2: (right) Color–color (UV−V versus V−I) diagram of the central 400 pc of NGC5253; each data point corresponds to a square bin about 10 pc in size. The colors shown have been subtracted for the underlying galaxy population and corrected for dust reddening. The curve represents the locus of models of constant star formation from Leitherer & Heckman (1995) and from Bruzual & Charlot (1995); representative model ages are marked.

Extinction–corrected color–color and color–EW(Hα) plots show that star formation has been an on-going process for the past ∼200 Myr, in the central ∼400 pc of NGC5253 (Figure 2). At present the peak of activity, identified with the Hα peak emission, is located in an area 50–60 pc in size right north of the dust lane, centered on NGC5253-5 (Figure 1). The area appears as young as ∼5 Myr, as suggested by the large EW(Hα) (Calzetti et al. 1997), the presence of W-R stars (Schaerer et al. 1997), the scarcity of red supergiants (Campbell & Terlevich 1984), and the purely thermal component of the radio emission (Beck et al. 1996); observations at radio wavelengths have revealed the presence of a dusty 'supernebula' in the area, possibly the youngest globular cluster known (Turner, Beck & Ho 2000). Although this is the most active region in the starburst, with a SFR∼20 $M_\odot$ yr^{-1}, it is not the UV-brightest: the area of peak activity is indeed rather dusty, likely still embedded in the parental molecular cloud with A_V ∼9–35 mag. The bulk of the observed UV emission is emerging

from the less active, relatively unextincted surrounding region, extending out to ∼200 pc in radius. This is the region where star formation has been going on at a relatively constant pace for ∼100–200 Myr, at the modest rate of 0.2 $M_\odot$ yr^{-1}. Apart for some evidence that star formation may be concentrating toward the center, thus moving inward, there is no other sign of a *spatial* evolution of the starburst in this galaxy.

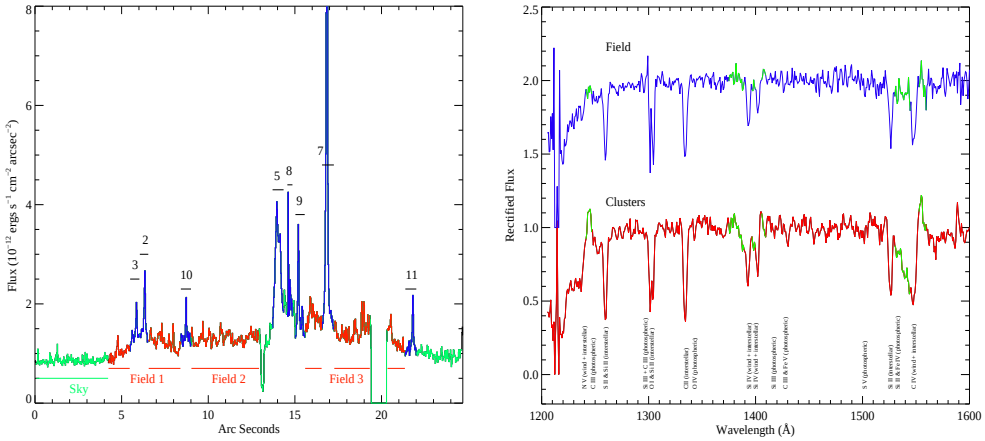

Figure 3: (left) A view of the NGC5253 emission collected by the STIS long slit, along the spatial direction. The figure shows the separate components that make up the UV emission of the starburst: stellar clusters (marked by numbers) and diffuse light (marked as 'Field'), that are well above the background (marked as 'Sky').

Figure 4: (right) The average cluster UV spectrum is compared with the average field UV spectrum. The two are markedly different; in particular the spectrum of the field lacks broad–line profiles in NV(1240 Å), SiIV(1400 Å), and CIV(1550 Å). This difference excludes scattered cluster light as source of the diffuse UV light (see the text and Tremonti et al. 2001 for a discussion of the nature of the diffuse light).

The long-slit of STIS was used to target a number of stellar clusters and the intracluster UV light in the center of NGC5253, and spectra in the wavelength range 1150–1700 Å were obtained (Figure 1 and Tremonti et al. 2001). Eight clusters fall within the STIS slit (Figure 3), while the diffuse light (marked as 'Fields' in Figure 3) covers a region of ∼220×1.9 pc^2 in total. The eight clusters have ages between 1 Myr and 8 Myr, and masses between a few 100 $M_\odot$ and 4×10^4 $M_\odot$. The mass of cluster NGC5253-5 is highly uncertain, depending on uncertain dust corrections, and could be as high as 6×10^5 $M_\odot$; possibly, the cluster coincides with the 'supernebula' detected in the radio by Turner et al. (2000).

The UV spectrum of the field is markedly different from the average spectrum of the stellar clusters, in that it lacks the broad–line profiles of NV, SiIV,

and CIV, characteristic of O-star winds (Figure 4). The diffuse UV light makes up between 50% and 80% of the total UV emission from local starburst galaxies (Buat et al. 1994; Meurer et al. 1995; Maoz et al. 1996); it has been suggested to originate from a mode of star formation that is separate from that of stellar clusters (Meurer et al. 1995). Comparison of the STIS UV spectra of the field with models indicate that, if the field population is produced by a separate mode of star formation from that of the clusters, this implies also a different IMF between the two. In particular, while the stellar clusters are compatible with a Salpeter (α=2.35) IMF in the range 1–100 $M_\odot$, the field population needs either a steeper-than-Salpeter IMF slope ($\alpha \sim$3.5) or a standard IMF slope with an upper mass cut-off at 30 $M_\odot$ (Tremonti et al. 2001). Steep IMF slopes have been found also for the field stars of the SMC and LMC, although the values are more extreme, $\alpha \sim$5, than those derived for NGC5253 (Massey et al. 1995). An alternative scenario to bimodal star formation is that of dissolving clusters. The field UV spectrum (Figure 4) is well modelled by a constant star formation synthetic spectrum from which the young stars' (younger than 10 Myr) contribution has been subtracted. This 'aged' constant model can easily account for the absence of the broad lines in NV, SiIV, and CIV, because the O–stars have been removed from it. According to this model, the lack of massive stars in the field is due to the lack of young stars. The clusters for which ages have been derived, either from spectroscopy or photometry, are typically younger than 10–20 Myr. If these are representative of the clusters' population in the starburst, clusters are generally younger than the field's stars. Thus, it is possible that *all stars form in clusters*, the clusters dissolve over a timescale of $\sim$10 Myr and their surviving stars disperse into the field. Models on the dissolution of compact stellar clusters in the center of galaxies (Kim, Morris & Lee 1999) predict that a 5×10^3 $M_\odot$ in NGC5253 evaporates in $\sim$15–20 Myr. This dissolution timescale is in the required ballpark to make the scenario consistent with the measured ages of NGC5253's clusters.

3. The Massive Galaxy NGC5236 (M83)

The starburst in M83 is harbored in a morphologically and dynamically complex central region (Figure 5). Located within the main bar of the galaxy, the center of M83 appears to contain a well-defined nuclear subsystem. The bright optical nucleus is offset from the center of the outer isophotes opposite to the starburst semi-annulus (Gallais et al. 1991), and a nuclear bar may separate the bright nucleus from the center (Elmegreen, Chromey & Warren 1998). The possible double nucleus suggests that another galaxy merged with M83 in the past; the merging event, together with the galaxy's bar, is a potential trigger of the current central starburst. Dense molecular gas is concentrated to the north of the starburst semi-annulus (Israel & Baas 2001), perhaps a result of material collecting around an inner Lindblad resonance, as suggested by Gallais et al. (1991). This cold material may be feeding the central starburst (Petitpas & Wilson 1998).

The starburst itself, in addition to be of comparable intensity to the event in NGC5253, is bright at all wavelengths, from the X-ray (Ehle et al. 1998), through the UV (Kinney et al. 1993), optical and near–IR (Gallais et al. 1991;

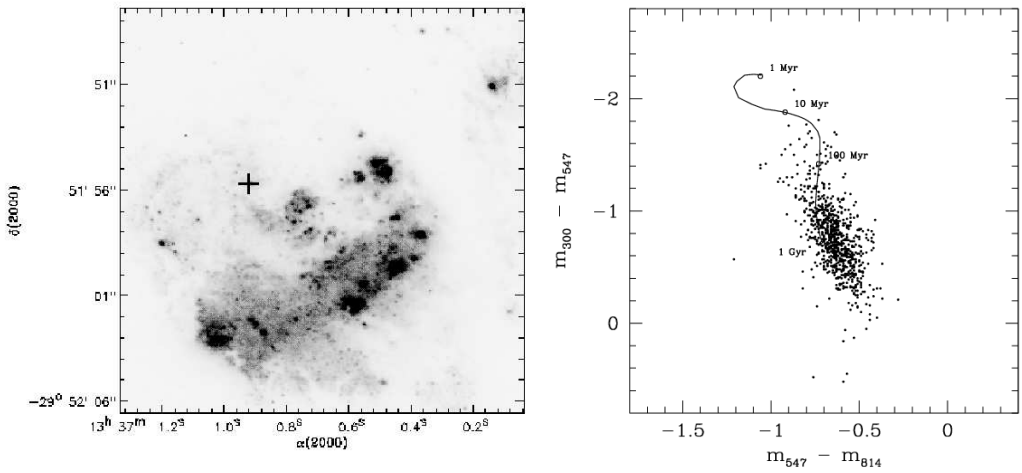

Figure 5:(left) The UV (2900 Å) WFPC2 image of the central region in NGC5236, showing the semi-annulus of active star formation and the position of the optical nucleus (marked with a cross). The nucleus is very bright at red wavelengths, but faint in the UV. A dark dust lane is located at the right edge of the image. The image has size 19″, which corresponds to a physical size of ∼360 pc. North is up, East is left.

Figure 6:(right) Color–color (UV−V versus V−I) diagram of the central 300 pc of M83; each data point corresponds to a square bin about 5 pc in size. The light from the 45 bright clusters, and from the underlying galaxy has been subtracted from the images prior to calculating these colors (that are also corrected for dust reddening). The curve represents the locus of models of constant star formation from Leitherer et al. (1999) at the appropriate metallicity for the galaxy; representative model ages are marked.

Rouan et al. 1996), through the mid–IR (Telesco et al. 1993), to the radio (Turner & Ho 1994). Multiple dust lanes cross the center of this metal–rich galaxy, although dust is very patchy, as demonstrated by the UV–brightness of the starburst semi-annulus (Figure 5). Two bright mid–IR sources, possibly two very young knots of star formation, are located at the NW edge of the starburst annulus, close to and/or embedded in a major dust lane (Telesco et al. 1993). The UV–bright region of star formation breaks down into almost 400 clusters brighter than m_{UV}=18 mag (Harris et al. 2001), while diffuse light represents more than 20% of the total UV emission. The Hα morphology closely follows that of the stellar emission, a different characteristic from NGC5253.

An analysis of the colors and EW(Hα) of the UV–bright population in M83, analogous to that performed for NGC5253 (see previous section), reveals that star formation has been continuous for the past ≈0.1–1 Gyr (Figure 6). This

is not dissimilar to what found in NGC5253, although a larger fraction of the population in M83 contains stars older than ∼500 Myr (Harris et al. 2001).

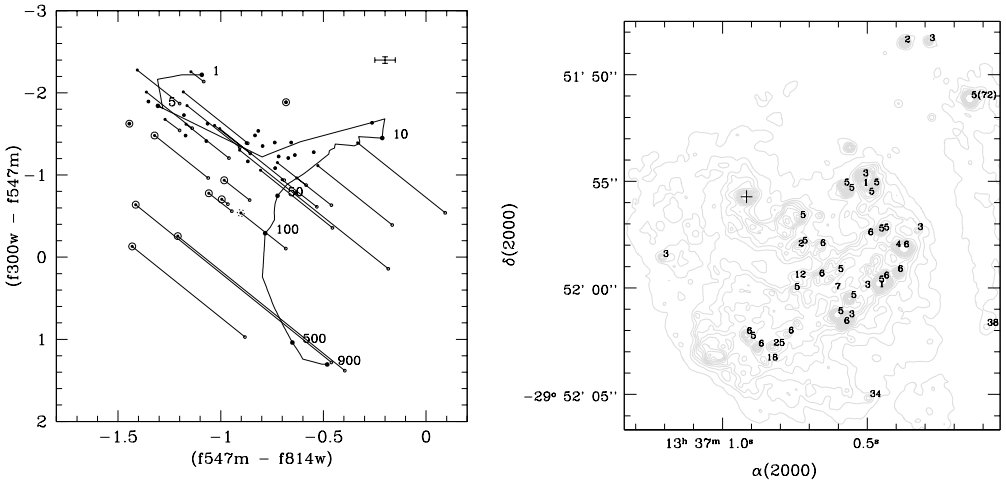

Figure 7: (left) Color–color (UV−V versus V−I) diagram of the 45 brightest clusters in M83. The observed colors are shown as empty circles; the dust-reddening corrected ones as filled circles. Lines connect the data points before and after reddening corrections. Filled circles with no connecting line are clusters located in areas of low or no reddening. Large empty circles with a central dot indicate clusters whose age could not be determined from colors; in these cases the EW(Hα) was used. The curve represents the locus of instantaneous burst models from Leitherer et al. (1999) at the appropriate metallicity for the galaxy; representative model ages are marked.

Figure 8: (right) A map of the cluster positions in M83; each cluster is marked by its age. The grey contours trace the V–band image and the position of the bright optical nucleus is indicated by a cross.

Among the ∼400 clusters detected in the UV with WFPC2, 45 are bright enough to be detected also in the shallower V and I images, enabling a study of their age and mass distributions (Harris et al. 2001). Again, colors and EW(Hα) were used as complementary diagnostics for the age of the stellar clusters (Figure 7). The basic result is that about 75% of the clusters more massive than 2×10^4 $M_\odot$ (our low mass completeness limit) are younger than 10 Myr, and almost 50% are in the narrow age range 5–7 Myr. No cluster older than ∼50 Myr was detected, although our images are deep enough for the purpose. While the 5–7 Myr old clusters are distributed across the semi-annulus of star formation, clusters younger than 5 Myr are preferentially located at the edges of the annulus (Figure 8). This suggests that star formation has propagated from the interior of the annulus to its perimeter. The 5–7 Myr population has possibly evacu-

ated interstellar material from most of the semi-annulus, and star formation is continuing along the edges, as also evidenced by the Hα morphology.

Along the semi-annulus, there is a trend for older clusters (ages around 10–30 Myr, Figure 8) to be located in the southern-most region, where the largest of the Hα bubbles is also located; whereas the peak of the current star formation is in the north-west area of the semi-annulus, close to a major dust lane and to the two mid-IR peaks (Telesco et al. 1993). This age sequence supports earlier suggestions that star formation has been propagating along the semi-annulus from the south to the north (Gallais et al. 1991; Puxley et al. 1997).

The full mass range for our clusters is $\sim 10^3$–8×10^4 $M_\odot$, and clusters more massive than a few times 10^4 $M_\odot$ are not expected to evaporate on timescales shorter than a few tens of Myr. Thus, the peak in the number of 5–7 Myr old clusters may suggest a true burst of activity in the recent past of the galaxy. This is consistent with evolution models already developed for the center of M83 (Gallais et al. 1991, Thatte et al. 2000): molecular gas is fed to the center by the main bar, and once enough mass is accumulated, star formation occurs. Typical sizes of the clouds would imply burst durations of 10–30 Myr (Efremov & Elmegreen 1998). Possibly, the current burst is a transitory flare-up of circumnuclear star formation, but if gas feeding of the center by the bar is recurrent or continuous, so would be the bursts of star formation. The absence of clusters older than 50 Myr in our images would suggest inter-burst periods >50 Myr.

A more accurate understanding of the star formation history in the center of M83 is currently hampered by our limitations in pinning down the nature of the diffuse UV light. This is mainly driven by the lack of UV spectroscopic data. For instance, if the UV spectra were to indicate that the diffuse population is mainly constituted of stars older than ≈50 Myr, this would reinforce the case for a true starburst nature of the 5–7 Myr old cluster population. A diffuse population containing signatures of young O–stars would support a bimodal star formation scenario (in contrast with NGC5253). Presence of field stars in the 10–50 Myr age range would re-open the question of whether the current starburst is a 'true burst' or simply part of a long duty-cycle event, because the scarcity of clusters older than ∼10 Myr could be ascribed to evaporation.

4. Conclusions

Preliminary results from the starburst star formation history project indicate that the morphological differences between the starbursts in the dwarf NGC5253 and in the massive spiral M83 may reflect differences in their history as well. In particular, the starburst in NGC5253 appears to be part of a time-extended (>100 Myr) event, while the starburst in M83 could be a 'true' burst of star formation, a short flare-up that could be separated from the next one by more than 50 Myr. The latter scenario is still under investigation, and UV spectroscopy will provide a final answer.

The next steps in the project include analysing the larger sample of starbursts, in order to place the above results on a solid statistical footing and address the questions posed in the Introduction.

D.C. thanks the Scientific Organizing Committee for the invitation to this stimulating and varied Conference in honor of our long-time friend and colleague Ken Freeman. This research was funded by the following grants: HST GO-8232, HST GO-8234, NASA NAG5-9173. Travel to the conference was funded by the STScI Director's Discretionary Research Funds.

References

Beck, S.C., Turner, J.L., Ho, P.T.P., Lacy, J.H., & Kelly, D.M. 1996, ApJ, 457, 610

Bruzual, G.A., & Charlot, S. 1995, private communication

Caldwell, N., & Phillips, M.M. 1989, ApJ, 338, 789

Calzetti, D., Meurer, G.R., Bohlin, R.C., Garnett, D.R., Kinney, A.L., Leitherer, C., & Storchi–Bergmann 1997, AJ, 114, 1834

Calzetti, D., Conselice, C.J., Gallagher, J.S., & Kinney, A.L. 1999, AJ, 118, 797

Campbell, A.W., & Terlevich, R. 1984, MNRAS, 211, 15

Cowie, L.L., Songaila, A., & Barger, A.J. 1999, AJ, 118, 603

Efremov, Y.N., & Elmegreen, B.G. 1998, MNRAS, 299, 588

Ehle, M., Pietsch, W., Beck, R., & Klein, U. 1998, A&A, 329, 39

Elmegreen, D.M., Chromey, F.R., & Warren, A.R. 1998, AJ, 116, 2834

Gallais, P. Rouan, D., Lacombe, F., Tiphene, D., & Vauglin, I. 1991, A&A, 243, 309

Harris, J., Calzetti, D., Gallagher, J.S., Conselice, C.J., & Smith, D.A. 2001, AJ, in press

Israel, F.P. & Baas, F. 2001, A&A, 371, 433

Kim, S.S., Morris, M., & Lee, H.M. 1999, ApJ, 525, 228

Kinney, A.L., Bohlin, R.C., Calzetti, D., Panagia, N., & Wyse, R.F.G. 1993, ApJS, 86, 5

Leitherer, C., & Heckman, T.M. 1995, ApJS, 96, 9

Leitherer, C., Schaerer, D., Goldader, J.D., et al. 1999, ApJS, 123, 3

Lilly, S.J., LeFevre, O., Hammer, F., & Crampton, D. 1996, ApJ, 460, L1

Maoz, D., Barth, A.J., Sternberg, A., Filippenko, A.V., Ho, L.C., Macchetto, F.D., Rix, H.-W., & Schneider, D.P. 1996, AJ, 111, 2248

Madau, P., Ferguson, H.C., Dickinson, M.E., Giavalisco, M., Steidel, C.C., & Fruchter, A. 1996, MNRAS, 283, 1388

Massey, P., Lang, C.C., Degioia-Eastwood, K., & Garmany, C.D. 1995, ApJ, 438, 188

Meurer, G.R., Heckman, T.M., Leitherer, C., Kinney, A.L., Robert, C., & Garnett, D.R. 1995, AJ, 110, 2665

Petitpas, G.R., & Wilson, C.D. 1998, ApJ, 503, 219

Puxley, P.J., Doyon, R., & Ward, M.J. 1997, ApJ, 476, 120

Rogstad, D.H., Lockhart, I.A., & Wright, M.C.H. 1974, ApJ, 193, 309

Rouan, D., et al. 1996, A&A, 315, L141

Sandage, A., Saha, A., Tamman, G.A., Labhardt, L., Schweneler, H., Panagia, N., & Macchetto, F.D. 1994, ApJ, 423, L13

Schaerer, D., Contini, T., Kunth, D., & Meynet, G. 1997, ApJ, 481, L75

Telesco, C.M., Dressel, L.L., & Wolstencroft, R.D. 1993, ApJ, 414, 120

Thatte, N., Tecza, M., & Genzel, R. 2000, A&A, 364, L47

Tremonti, C.A., Calzetti, D., Leitherer, C., & Heckman, T.M. 2001, ApJ, 555, 322

Turner, J.L., Beck, S.C., & Ho, P.T.P. 2000, ApJ, 532, L109

Turner, J.L., & Ho, P.T.P. 1994, ApJ, 421, 122

Turner, J.L., Ho, P.T.P., & BECK, S.C. 1998, AJ, 116, 1212

van den Bergh, S. 1980, PASP, 92, 122

Walborn, N.R., Barbá, R.H., Brandner, W., Rubio, M., Grebel, E.K., & Probst, R.G. 1999, AJ, 117, 225